

## Chapter II

### **An Isotopic Tracer Study of the Deactivation of Ru/TiO<sub>2</sub> Catalysts During Fischer-Tropsch Synthesis**

#### ABSTRACT

An investigation of the causes of catalyst deactivation during Fischer-Tropsch synthesis over Ru/TiO<sub>2</sub> catalysts has been carried out. The effects of Ru dispersion, TiO<sub>2</sub> phase, and TiO<sub>2</sub> surface area on catalyst activity and selectivity were examined. CO chemisorption capacity and carbon species accumulation were determined as a function of reaction time using isotopic tracer techniques in conjunction with temperature-programmed surface reaction (TPSR). The results of this investigation show that all of the catalysts undergo deactivation with time, with no change in product selectivity. Initially, deactivation is very rapid followed by a slower activity loss. The long-term rate of deactivation is proportional to the initial CO turnover frequency, obtained by extrapolation of the long-term activity data. Deactivation is accompanied by a progressive loss in CO chemisorption capacity as well as an accumulation of various types of carbon species. Carbidic carbon, C<sub>α</sub>, and alkyl carbon chains, C<sub>β</sub>, were observed to accumulate as reaction proceeds. C<sub>β</sub> consists of two species, C<sub>β</sub>' which is the precursor to C<sub>2+</sub> hydrocarbon products and C<sub>β</sub>" which

consists of longer alkyl chains and does not participate in the production of gas phase products. The rapid initial loss in activity in the first ten minutes correlates with the  $C_{\alpha}+C_{\beta}$  accumulation; the long-term loss in CO uptake and catalyst activity are probably due to  $C_{\beta}$ . The alkyl chains comprising  $C_{\beta}$  do not undergo hydrogenolysis under reaction conditions, probably due to inaccessibility to hydrogen.

## INTRODUCTION

A number of previous investigations have shown that while Ru exhibits a high specific activity for Fischer-Tropsch synthesis, it undergoes a progressive loss in activity that is accompanied by a build-up of carbonaceous species (1-6). Dalla Betta and co-workers (1,2) have ascribed the loss in activity of Ru/Al<sub>2</sub>O<sub>3</sub> catalysts to the carbonaceous deposits, and have noted that the original activity of these catalysts could be restored by reduction in H<sub>2</sub>. Similar observations have been reported by Everson *et al.* (3) and Ekerdt and Bell (4). These authors noted that the rate of deactivation was a function of reaction conditions. Using infrared spectroscopy, Ekerdt and Bell (4) and Yamasaki and co-workers (7) observed the accumulation of hydrocarbon species on the surface under reaction conditions. Ekerdt and Bell (4) concluded that the observed species did not function as reaction intermediates, since these species could only be removed by H<sub>2</sub> reduction in the absence of CO. Reduction of the catalyst following reaction demonstrated that during reaction, the catalyst had accumulated 1-6 Ru ML equivalents of carbon. Based on studies on a Ru/Al<sub>2</sub>O<sub>3</sub> catalyst, Bartholomew *et al.* (6) have proposed a model for the rate of deactivation. According to this model, the rate of deactivation is proportional to the partial pressure of CO and the concentration of active sites. Temperature programmed reaction of the catalyst after reaction produced a spectrum exhibiting two peaks. The first of these peaks occurred at 460 K and corresponded to the removal of 5 ML equivalents of

carbon, whereas the second peak occurred at 685 K and corresponded to the removal of 2.5 ML equivalents of carbon.

Isotopic tracer studies conducted in this laboratory (8-14) have demonstrated that two types of carbon are deposited on the surface of Ru particles supported on  $\text{SiO}_2$  and  $\text{TiO}_2$ . The first is carbidic, or  $\text{C}_\alpha$ , carbon. This species is produced by the dissociation of adsorbed CO and serves as a precursor to methane and  $\text{C}_{2+}$  hydrocarbons. The second form of carbon consists of short (3-5 carbon atoms) alkyl chains and is designated as  $\text{C}_\beta$ . By combining isotopic tracer techniques with temperature programmed reaction, it has been shown that the  $\text{C}_\beta$  pool of carbon can be divided into two pools. The first of these pools is designated as  $\text{C}_\beta'$ , and corresponds to alkyl groups serving as intermediates to the  $\text{C}_{2+}$  hydrocarbons. The second pool of carbon, designated as  $\text{C}_\beta''$ , corresponds to longer alkyl chains which are not involved in the formation of reaction products. Under reaction conditions, the coverages of  $\text{C}_\alpha$  and  $\text{C}_\beta'$  come to a steady state with time, whereas the accumulation of  $\text{C}_\beta''$  increases monotonically. Zhou and Gulari (15) have also found evidence for the presence of  $\text{C}_\alpha$  and  $\text{C}_\beta$  during CO hydrogenation over  $\text{Al}_2\text{O}_3$ -supported Ru. The inventory of  $\text{C}_\alpha$  was observed to go through a maximum with reaction time, whereas the inventory of  $\text{C}_\beta$  increased monotonically. In a subsequent study (16), the authors speculated that the low activity alkyl species that could be observed by infrared spectroscopy were located on sites surrounded

by adsorbed CO.

The objective of this study was to characterize the deactivation of Ru/TiO<sub>2</sub> catalysts during Fischer-Tropsch synthesis and to identify the causes for the loss in activity. The influence of Ru dispersion, TiO<sub>2</sub> phase, and TiO<sub>2</sub> surface area were considered. The CO chemisorption capacity and the quantity of carbon accumulated were determined as a function of time under reaction conditions. Isotopic tracer techniques were used in conjunction with temperature-programmed surface reaction (TPSR) to study changes in the reactivity of CO and the different forms of carbon accumulated on the catalyst.

## EXPERIMENTAL

Four titania supports were used for this study: Degussa P-25 titania, a mixture of 30% rutile and 70% anatase; two anatase supports differing in BET surface area; and rutile. These supports will be referred to as TiO<sub>2</sub>(D), TiO<sub>2</sub>(A1), TiO<sub>2</sub>(A2), and TiO<sub>2</sub>(R). TiO<sub>2</sub>(A1) is the higher surface area anatase.

TiO<sub>2</sub>(A1) was prepared as follows. Titanium isopropoxide (Ti(C<sub>3</sub>H<sub>7</sub>O)<sub>4</sub>, Dupont) was added dropwise to an excess of isopropyl alcohol at 274 K over a period of 4.5 hours with constant mixing. The resulting slurry was allowed to settle, decanted and washed with distilled water. The decanting and washing was repeated 5-6 times, and the slurry was then filtered and washed several times. The final product was ground and calcined in an O<sub>2</sub> atmosphere. The

preparation of  $\text{TiO}_2(\text{A2})$  was similar to that of  $\text{TiO}_2(\text{A1})$ , except that the initial step was carried out at 280 K.

$\text{TiO}_2(\text{R})$  was prepared according to the procedure described by Kikuchi *et al.* (16). Titanium tetrachloride ( $\text{TiCl}_4$ ) was added dropwise to hot distilled water at 368K, stirred for 1 hour, and then cooled to ambient temperature. After filtration, precipitated titanium hydroxide was washed with distilled water and filtered again. The washing cycle was repeated several times and finally the precipitate was dried overnight at 383 K. To remove residual chloride impurities, the support was Soxhlet extracted with water and then calcined in pure  $\text{O}_2$  at 673 K. Extraction and calcination were repeated three times (18).

The phase structure of each  $\text{TiO}_2$  support was confirmed using Raman spectroscopy, since this technique is very sensitive to the phase of  $\text{TiO}_2$  and can detect small proportions of anatase in the presence of rutile. By this means, it was established that  $\text{TiO}_2(\text{R})$  contained no traces of anatase and that  $\text{TiO}_2(\text{A1})$  and  $\text{TiO}_2(\text{A2})$  contained no detectable traces of rutile.

Ru was introduced onto each support by incipient wetness impregnation using an aqueous solution of  $\text{RuCl}_3 \cdot 3\text{H}_2\text{O}$  (Strem). The impregnated supports were dried in air at 373 K overnight, and then sieved to -30, +60 mesh. Reduction of the dried products were carried out at 503 K in a flow of pure  $\text{H}_2$ . The reduction temperature was intentionally kept low to keep the catalyst in its low-temperature reduced state as much as possible (19). To check for complete conversion of the  $\text{RuCl}_3$  to metallic Ru, the chloride

content of each catalyst was determined after reduction. The chloride level in Ru/TiO<sub>2</sub>(D) and Ru/TiO<sub>2</sub>(A1) was below the detection limit (0.02%). For Ru/TiO<sub>2</sub>(A2) and Ru/TiO<sub>2</sub>(R), the levels were 0.04% and 0.07% respectively. The weight loading of Ru was determined by X-ray fluorescence.

Table 1 summarizes the physical characteristics of each catalyst. The dispersion of the Ru was determined by H<sub>2</sub> chemisorption at 373 K following a two hour reduction at 473 K. Chemisorption was carried out at 373 K because hydrogen adsorption is known to approach equilibrium slowly at room temperature (20), and equilibrium is attained more rapidly at this temperature (21, 22). A static chemisorption apparatus was used. The isotherms for total and reversible adsorption were determined and the difference between the intercepts at zero pressure was used to estimate hydrogen uptake. The CO chemisorption capacity of Ru was determined by temperature programmed surface reaction in D<sub>2</sub> following reduction at 498 K in pure D<sub>2</sub> for two hours. Further details concerning this procedure are discussed in the Results section. The BET surface area and pore size distribution for each catalyst was determined from N<sub>2</sub> isotherms at 77K.

H<sub>2</sub>, CO and He were supplied from a gas flow manifold to a low dead volume quartz microreactor. UHP H<sub>2</sub> (Matheson Gas) or D<sub>2</sub> supplied by U.C.L.B.L. were further purified by passage through a Deoxo unit (Engelhard Industries) and water was removed by a molecular sieve 13X trap. UHP CO (99.999% pure, Matheson Gas) was passed through a glass bead trap at 573 K to remove iron carbonyls,

Table 1

## Catalyst characteristics

Catalyst	Ru (wt %)	Dispersion (%)	BET (m <sup>2</sup> /gm)	H uptake (μmoles/gm)	CO/H	pore dia (Å)
Ru/TiO <sub>2</sub> (D)	3.3	15.5	47.5	51.1	1.3	213
Ru/TiO <sub>2</sub> (A1)	3.7	30.9	105.4	112.5	0.8	94
Ru/TiO <sub>2</sub> (A2)	3.1	40.6	76.5	125.3	0.8	120
Ru/TiO <sub>2</sub> (R)	6.1	30.8	46.0	186.6	2.2	167



an Ascarite trap to remove CO<sub>2</sub>, and finally a molecular sieve trap. UHP He was passed through a molecular sieve trap. 99% <sup>13</sup>CO (Isotec Inc) was used as supplied.

The products of CO hydrogenation were analysed by gas chromatography using a Perkin Elmer Sigma 3B gas chromatograph equipped with a FID detector. C<sub>1</sub>-C<sub>14</sub> hydrocarbons were separated on a fused silica capillary column (0.25 mm i.d. x 50m) coated with SE-54 (1 μm thick). Temperature programming of the column was as follows: 253 K for 5 min, 20 K/min upto 523 K, and then 523K for 10 min. Since the analysis of each loop requires 28.5 min, samples of reaction products were taken as needed, stored at 393 K, and then introduced to the chromatograph after reaction. To accomplish this, the effluent from the reactor was routed through a 10-port, two-position valve (used either to sample the products or inject the stored sample into the chromatograph) in series with a 16 sample-loop multiposition valve (used to acquire and store the samples). Both valves were contained in heated ovens maintained at 393 K to avoid condensation of products. Operation of both valves was by motor-driven actuators connected to a personal computer (IBM-PC). The microcomputer was programmed to schedule sample acquisition and analysis at desired times. The output from the FID detector was acquired by the computer via an interface and stored at a rate of 2 data points per second.

During a temperature-programmed surface reaction experiment, the reactor effluent was monitored by a mass spectrometer (UTI 100C). The following masses were monitored: 15

( $^{12}\text{CH}_4$ ), 21 ( $^{13}\text{CD}_4$ ), 28 ( $^{12}\text{CO}$ ), 29 ( $^{13}\text{CO}$ ), 44 ( $^{12}\text{CO}_2$ ) and 45 ( $^{13}\text{CO}_2$ ). Mass spectrometer control and data acquisition were carried out by the personal computer. Using this system each mass intensity could be sampled twice a second.

For each experiment, 0.2 to 0.3 gm of catalyst was loaded in the reactor. The catalyst was then reduced by slowly ramping the temperature in  $\text{D}_2$  at 10 K/min to 503 K, and then holding at this temperature for at least two hours. The synthesis of hydrocarbons was carried out at 1 atm using  $^{12}\text{CO}$  and  $\text{D}_2$ . All reactions were performed at the following conditions:  $T = 498\text{K}$ ;  $\text{D}_2/\text{CO} = 3$ ;  $P_{\text{CO}} = 50$  torr;  $P_{\text{D}_2} = 150$  torr;  $P_{\text{He}} = 560$  torr;  $Q = 150$  cc/min. CO conversions on all the catalysts were  $< 10\%$ . Activity was followed as a function of reaction time ( $t_r$ ) by sampling at different times after the start-up of the reaction, and data were collected up to four hours onstream. After reaction, the catalyst was reduced at 503 K overnight.

TPSR experiments were initiated by pretreating the catalyst in one of several ways, as discussed in the Results section. The reactor was flushed with He to remove gas phase reactants and the catalyst was quenched in He to room temperature in under one minute by blowing air over the outside of the reactor. If the uptake of CO was to be determined, the catalyst was exposed to 50 torr of  $^{13}\text{CO}$  in He for 5 min, and then flushed in pure He. The final step in each TPSR experiment was to ramp the catalyst temperature at 0.17 K/s to 503 K in flowing  $\text{D}_2$  (50 torr). During this period, the evolution of  $^{13}\text{C}$  labeled products (including  $^{13}\text{CO}$  and  $^{13}\text{CD}_4$ ) was

monitored by the mass spectrometer.

## RESULTS

Figure 1 shows a plot of the turnover frequency for CO conversion to hydrocarbons,  $N_{CO}$ , as a function of time under reaction conditions, for each of the four catalysts.  $N_{CO}$  was determined by summing the rate of formation of  $C_1$  through  $C_{14}$  hydrocarbons weighted by the carbon number and dividing this sum by the moles of surface Ru atoms determined by hydrogen chemisorption. Each of the catalysts exhibits a rapid initial loss in activity which is then followed by a much slower decline. The initial activity could be restored by  $D_2$  reduction at 498 K and the plots of  $N_{CO}$  versus time could be reproduced over several cycles of reduction and reaction. It was also observed that the room temperature uptake of CO after reduction of the partially deactivated catalysts was identical to that prior to reaction.

The initial activity at  $t_r = 1$  min for  $Ru/TiO_2(D)$ ,  $Ru/TiO_2(A1)$  and  $Ru/TiO_2(A2)$  exhibits an inverse linear correlation with Ru dispersion, as shown in Fig. 2. The point for  $Ru/TiO_2(R)$  lies well below the correlation. For  $t_r > 20$  min, the loss in activity can be fit by an exponential function,  $N_{CO} = N_{CO}^0 \exp(-t_r/\tau)$ , where  $N_{CO}^0$  is the apparent initial activity at  $t_r = 0$  min and  $\tau$  is the time constant for deactivation. The values of  $\tau$  are 310 min for  $Ru/TiO_2(D)$ , 420 min for  $Ru/TiO_2(A1)$ , 500 min for  $Ru/TiO_2(A2)$  and 714 min for

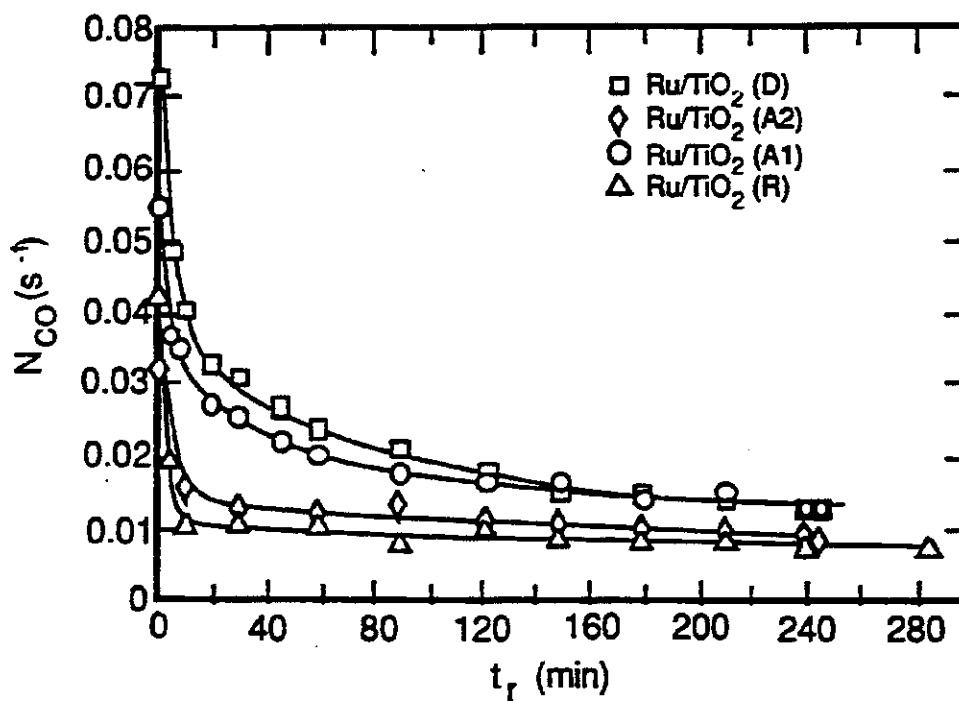


Fig. 1 CO turnover frequency as a function of reaction time. Reaction Conditions:  $P_{D_2} = 150$  torr,  $P_{CO} = 50$  torr,  $T = 498$  K.

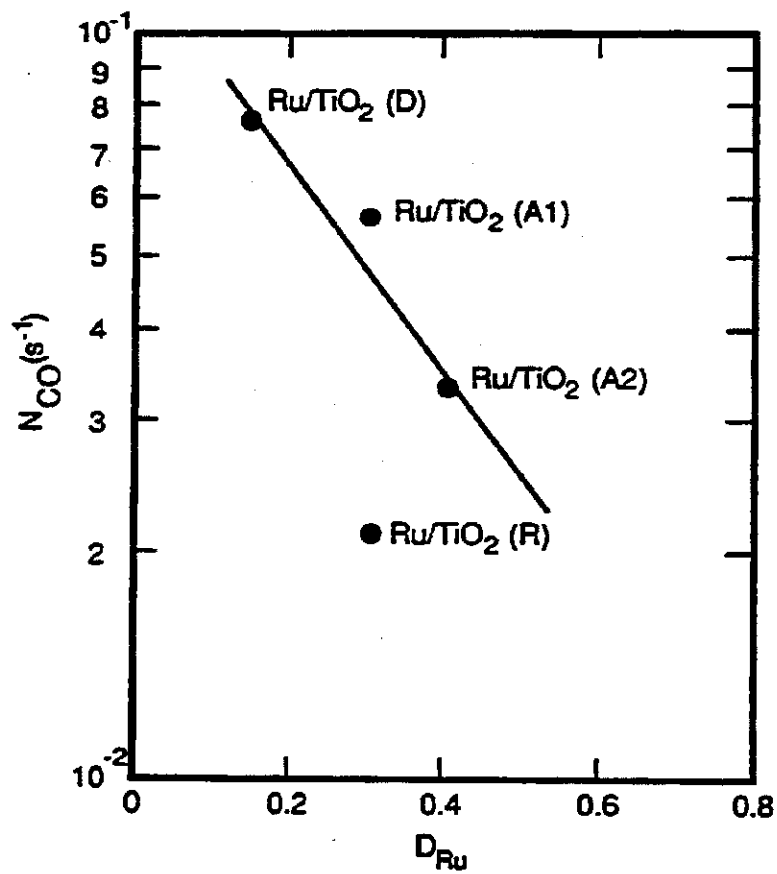


Fig. 2 Catalyst activity at 1 min after reaction start up versus ruthenium dispersion.

Ru/TiO<sub>2</sub>(R). Figure 3 shows that a linear correlation exists between  $\tau^{-1}$  and  $N_{CO^0}$ , which suggests that whatever causes the slow deactivation of the catalyst is produced by the catalyst itself.

Figure 4 shows an Anderson-Schulz-Flory (23) plot of the distribution of C<sub>1</sub> through C<sub>14</sub> hydrocarbons for  $t_r = 5$  min and  $t_r = 120$  min for Ru/TiO<sub>2</sub>(D). It is evident that the carbon number distribution of products is not strongly affected by deactivation. Similar observations were also made for the other three catalysts. Moreover, for all four catalysts, the probability of chain growth,  $\alpha$ , was found to be  $0.7 \pm 0.01$ , indicating that  $\alpha$  is independent of Ru dispersion and support properties (i.e., TiO<sub>2</sub> phase and surface area). The effects of reaction time on the proportions of total olefins, internal olefins, and branched products was examined at each carbon number between 2 and 7. For a given carbon number, the fraction of  $\alpha$ -olefins was observed to rise during the first 10 min, at the same time that the fraction of  $\beta$ -olefins declined by an equivalent amount; however, neither the proportion of total olefins nor the proportion of branched products changed significantly with reaction time.

The CO adsorption capacity of each catalyst was measured both prior to the onset of reaction and after progressively longer periods of time under reaction conditions. The CO uptake of a freshly reduced catalyst was determined by exposing it to <sup>13</sup>CO at room temperature for 5 min, flushing the catalyst with He for 15 min and then carrying out a temperature-programmed surface reaction in D<sub>2</sub>. A peak of <sup>13</sup>CD<sub>4</sub> was observed. To estimate the CO

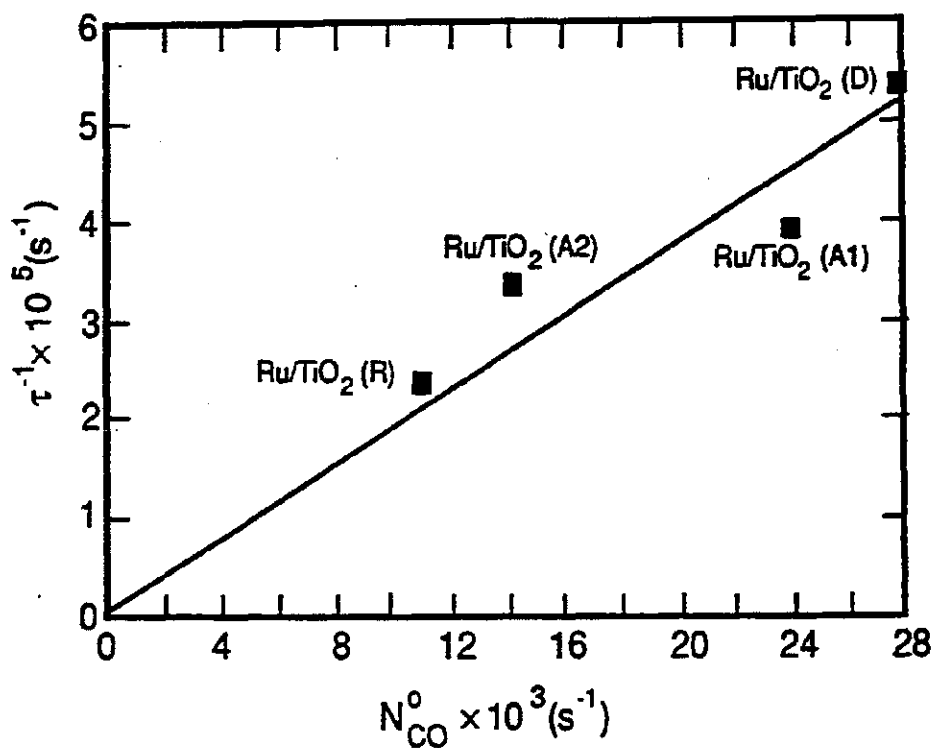


Fig. 3 Correlation of the inverse of the deactivation time constant with the CO turnover frequency at  $t_r = 0$  obtained by extrapolation of the  $N_{\text{CO}}$  versus  $t_r$  curve for  $t_r \geq 20$  min.

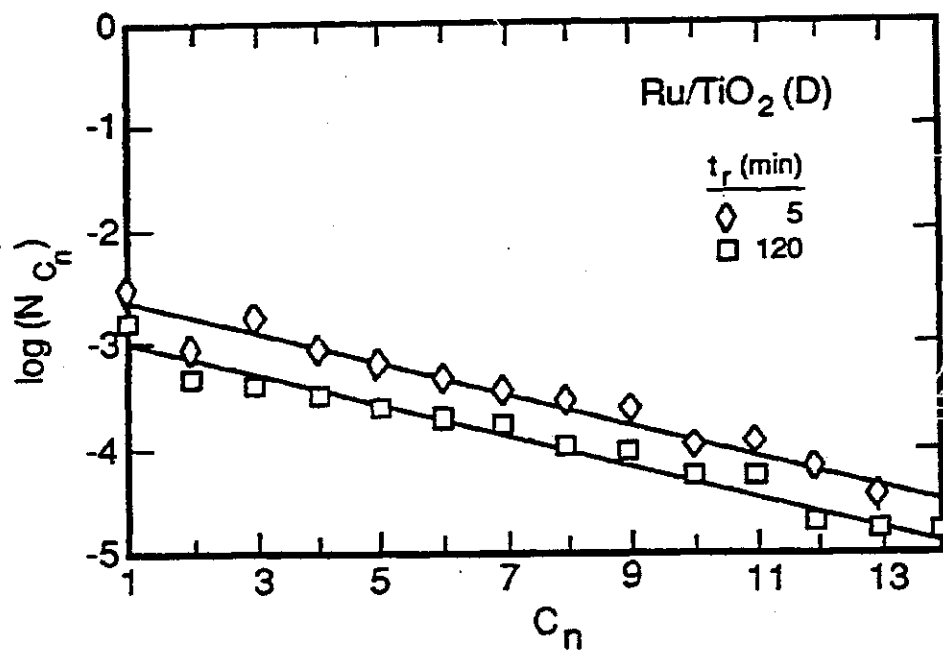


Fig. 4 Effect of reaction time on the ASF plot ( $\log N C_n$  vs  $C_n$ ) for Ru/TiO<sub>2</sub>(D).  $N C_n$  is the turnover frequency for products of carbon number  $n$ .



adsorption capacity after reaction, reaction was carried out in a mixture of  $^{12}\text{CO}/\text{D}_2$  for a specified time after which the catalyst was cooled abruptly to room temperature in flowing He. The  $^{12}\text{CO}$  remaining on the catalyst surface was displaced by exposing the catalyst to  $^{13}\text{CO}$  for 5 min. The catalyst was then flushed in He for 15 min and a temperature-programmed surface reaction was carried out in flowing  $\text{D}_2$ .

The only  $^{13}\text{C}$ -labeled product observed during the temperature-programmed surface reaction of adsorbed  $^{13}\text{CO}$  was  $^{13}\text{CD}_4$ . As can be seen in Fig. 5, the amount of  $^{13}\text{CD}_4$  formed decreases with increasing  $t_r$ . This change is accompanied by a progressive upscale shift in the temperature of the maximum rate of  $^{13}\text{CD}_4$  formation. It is also apparent, particularly for  $\text{Ru}/\text{TiO}_2(\text{R})$ , that the  $^{13}\text{CD}_4$  spectrum for  $t_r > 0$  consists of two or more overlapping peaks. The apparent activation energy for the reduction of adsorbed  $^{13}\text{CO}$  was estimated from a plot of the log of the initial rate of  $^{13}\text{CD}_4$  formation versus inverse temperature. A value of  $30 \pm 2.5$  kcal/mol was obtained for all of the catalysts, independent of  $t_r$ .

The area under the  $^{13}\text{CD}_4$  peaks obtained during temperature-programmed surface reaction of  $^{13}\text{CO}$  is taken as the measure of the CO adsorption capacity of Ru. Figure 6 shows that as  $t_r$  increases, the CO adsorption capacity of each of the four catalysts decreases rapidly and then declines more slowly for  $t_r \geq 5$  min. As can be seen from Table 2, the time constants for the slow loss of CO adsorption capacity are virtually identical to those for the slow loss in CO hydrogenation activity.

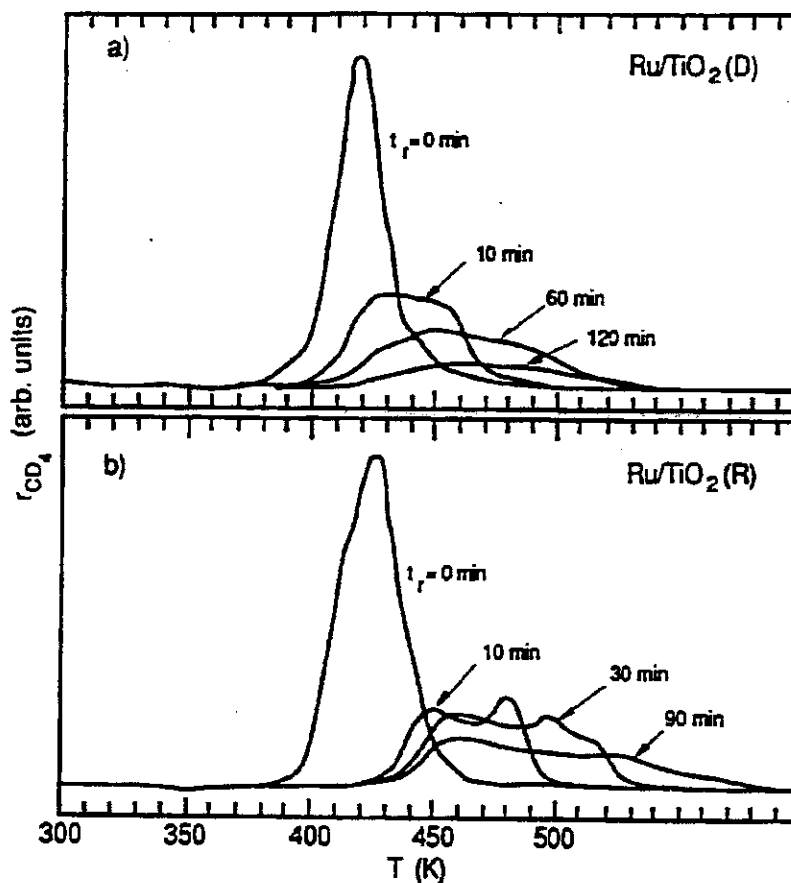


Fig. 5  $^{13}\text{C}$  TPSR spectra to estimate CO uptake as a function of  $t_r$ . a. Data for  $\text{Ru/TiO}_2(\text{D})$ . b. Data for  $\text{Ru/TiO}_2(\text{R})$ .

Reaction Conditions:  $P_{\text{D}_2} = 150$  torr,  $P_{\text{CO}} = 50$  torr,  $T = 498$  K. Gas Introduction sequence:  $^{12}\text{CO} + \text{D}_2 (t_r) \rightarrow \text{He (cool)} \rightarrow ^{13}\text{CO} (5 \text{ min}) \rightarrow \text{D}_2$  (TPSR). In the TPSR spectra, the temperature is raised from room temperature to 503 K at 0.17 K/sec and then maintained constant at 503 K.

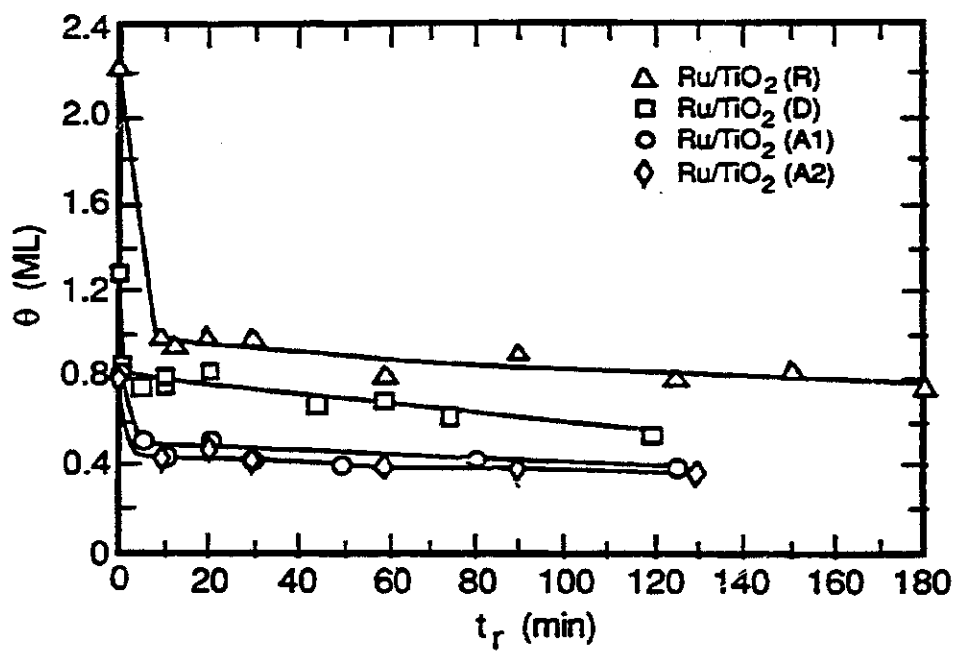


Fig. 6 CO uptake as a function of reaction time,  $t_r$ .

Table 2

Comparison of the time constants for the decay in  $N_{CO}$  with that for the decay in  $\theta_{CO}$ , for  $t_r > 20$  min

Catalyst	$N_{CO}$ decay (min)	$\theta_{CO}$ decay (min)
Ru/TiO <sub>2</sub> (D)	310	306
Ru/TiO <sub>2</sub> (A1)	420	476
Ru/TiO <sub>2</sub> (A2)	500	550
Ru/TiO <sub>2</sub> (R)	714	715

Additional experiments were performed to determine the cause of the immediate loss of CO chemisorption capacity upon initiation of CO hydrogenation. The freshly reduced catalyst was exposed to  $^{13}\text{CO}$  at room temperature for 5 min, flushed in He for 5 min, and then contacted with  $^{12}\text{CO}$  in He for 5 min to exchange off all the adsorbed  $^{13}\text{CO}$ . The catalyst was then flushed with He and TPSR in  $\text{D}_2/\text{He}$  was initiated. A pulse of  $^{13}\text{CO}_2$  was observed when the catalyst contacted with  $^{13}\text{CO}$ , and a peak of  $^{13}\text{CD}_4$  was observed during TPSR. Both of these observations suggest that some of the adsorbed  $^{13}\text{CO}$  disproportionates via the reaction:  $2\text{CO}_s \rightarrow \text{C}_s + \text{CO}_2(\text{g})$ . As shown in Table 3, the amount of  $^{13}\text{C}_s$  deposited by CO disproportionation correlates well with the immediate loss of CO chemisorption capacity observed upon initiation of CO hydrogenation over  $\text{Ru}/\text{TiO}_2(\text{D})$ ,  $\text{Ru}/\text{TiO}_2(\text{A1})$ , and  $\text{Ru}/\text{TiO}_2(\text{A2})$ . Similar results have been reported by Yamasaki *et al.* (7) who observed that CO disproportionation caused a reduction in the extent of CO adsorption. For  $\text{Ru}/\text{TiO}_2(\text{R})$ , the loss in CO chemisorption capacity is much greater than the amount of carbon deposited by room-temperature disproportionation of CO. It is also observed that the amount of carbon deposited on  $\text{Ru}/\text{TiO}_2(\text{R})$  by CO disproportionation is significantly less than that deposited on the other three catalysts.

The accumulation of carbonaceous species on the catalyst was determined using the following procedure. Reaction was run for a specified duration using a feed mixture of  $^{13}\text{CO}$  and  $\text{D}_2$ . The catalyst was then exposed for 30 s to  $^{12}\text{CO}$  in He, to exchange the adsorbed  $^{13}\text{CO}$  for  $^{12}\text{CO}$  (13), after which the catalyst was rapidly cooled to

Table 3

Comparison of the initial Loss in  $\theta_{CO}$  with that due to room temperature disproportionation of CO

Catalyst	Loss on running reaction (ML)	Room Temp. disprop. CO (ML)
Ru/TiO <sub>2</sub> (D)	0.45	0.47
Ru/TiO <sub>2</sub> (A1)	0.33	0.27
Ru/TiO <sub>2</sub> (A2)	0.35	0.34
Ru/TiO <sub>2</sub> (R)	1.23	0.13

room temperature in flowing He. Temperature-programmed surface reaction was then carried out in flowing  $D_2$  and the formation of  $^{13}CD_4$  was monitored as a function of time. Spectrum b in Fig. 7 shows the rate of  $^{13}CD_4$  formation versus the temperature for the case of Ru/TiO<sub>2</sub>(D). Spectrum a shows the rate of  $^{13}CD_4$  formation if the exchange of adsorbed  $^{13}CO$  for  $^{12}CO$  is eliminated from the procedure. The area under spectrum b corresponds to the total amount of carbonaceous species present on the catalyst, namely, the sum of  $C_\alpha$  and  $C_\beta$ , whereas the area under spectrum a also includes the amount of chemisorbed CO.

As discussed by Yokomizo et al. (14), the  $C_\beta$  pool of carbon can be subdivided into two pools: a  $C_\beta'$  pool corresponding to alkyl precursors to  $C_{2+}$  products and a  $C_\beta''$  pool corresponding to alkyl groups produced by reaction, but not associated with the formation of  $C_{2+}$  products. The amount of  $C_\beta''$  was determined using the following procedure. The reaction was run in a mixture of  $^{13}CO$  and  $D_2$  for a time  $t_r$ . The feed was then switched to a mixture of  $^{12}CO$  and  $D_2$  for 2 min. Experiments performed to determine the reaction time required for the latter step showed that within 2 min, the adsorbed  $^{13}CO$  would be displaced by  $^{12}CO$  and all the  $^{13}$ -labeled carbon in the  $C_\alpha$  and  $C_\beta'$  pools would be replaced by  $^{12}C$ , but that the  $^{13}C$  carbon in the  $C_\beta''$  pool would remain. After reaction in the  $^{12}CO/D_2$  mixture, the catalyst was rapidly cooled to room temperature in He, and a temperature-programmed surface reaction

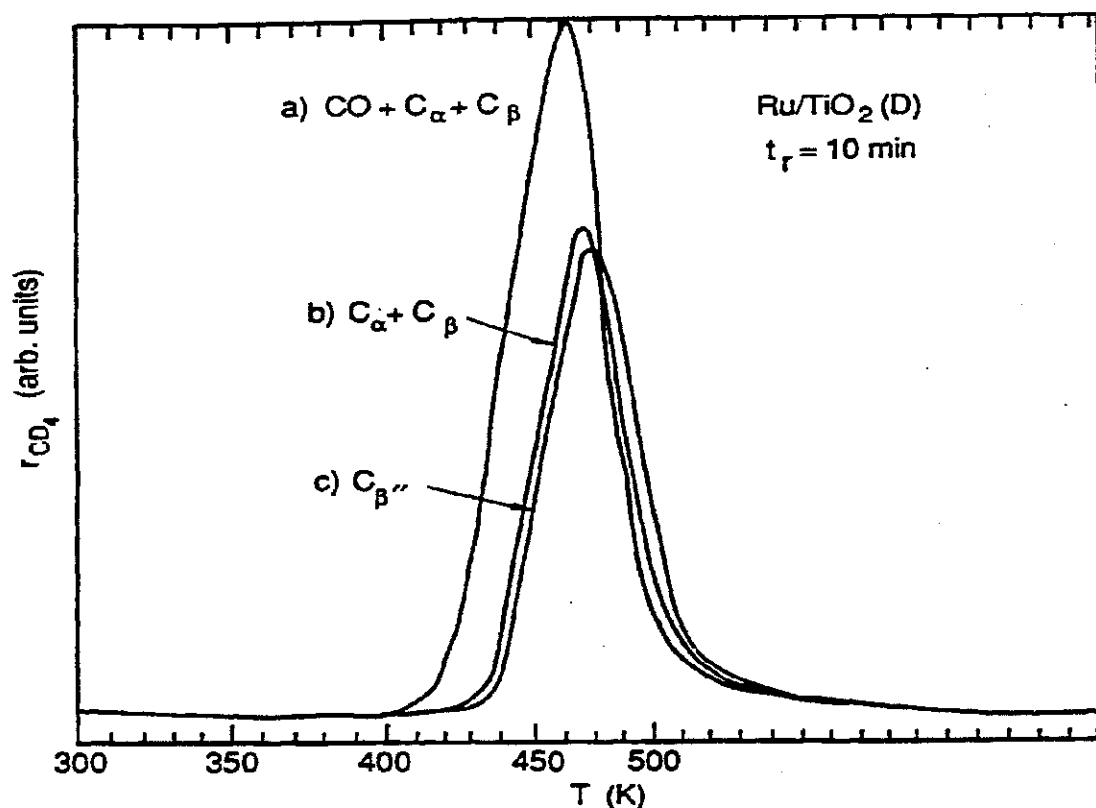


Fig. 7  $^{13}\text{C}$  TPSR spectra to estimate carbon accumulation on the catalyst at  $t_r = 10$  min, standard reaction conditions. a. CO + C<sub>α</sub> + C<sub>β</sub>. Gas Introduction sequence:  $^{13}\text{CO} + \text{D}_2$  (10 min) → He (cool) → D<sub>2</sub> (TPSR). b. C<sub>α</sub> + C<sub>β</sub>: Gas Introduction sequence:  $^{13}\text{CO} + \text{D}_2$  (10 min) →  $^{12}\text{CO} + \text{He}$  (30 s) → He (cool) D<sub>2</sub> (TPSR). c. C<sub>β</sub>''. Gas Introduction sequence:  $^{13}\text{CO} + \text{D}_2$  (10 min) →  $^{12}\text{CO} + \text{D}_2$  (2 min) → He (cool) → D<sub>2</sub> (TPSR). In the TPSR spectra, the temperature is raised from room temperature to 503 K at 0.17 K/sec and then maintained constant at 503 K.



was then carried out in flowing  $D_2$ . Spectrum c in Fig. 7 shows the resulting trace of  $^{13}CD_4$  formation as a function of temperature. The small difference in the areas under spectra c and b represents the amount of  $C_{\alpha}+C_{\beta}'$  carbon accumulated on the catalyst. Figure 8 shows that the amount of  $C_{\beta}''$  builds up monotonically as  $t_r$  increases.

The accumulation of  $C_{\alpha}$ ,  $C_{\beta}'$ , and  $C_{\beta}''$  during the first 20 min of reaction are shown in Fig. 9. It is evident that the surface concentration of  $C_{\alpha}$  and  $C_{\beta}'$  is less than 1 ML in most cases. For Ru/TiO<sub>2</sub>(R), RuTiO<sub>2</sub>(A1) and Ru/TiO<sub>2</sub>(D), the accumulation of these forms of carbon passes through a maximum as  $t_r$  increases. Much larger quantities of  $C_{\beta}''$  are formed on the catalyst surface and these species increase in quantity monotonically, and after 20 min of reaction can be as high as 7 ML equivalents. The time constant for the build up of  $C_{\alpha}+C_{\beta}$  during the first 10 min of reaction is listed in Table 4 and is compared with the time constant for the loss in CO hydrogenation activity during the same period. It is apparent that the time constants for the two phenomena are virtually identical, suggesting that the loss in CO hydrogenation activity during the initial stages of reaction can be attributed to the rapid buildup of  $C_{\alpha}$  and  $C_{\beta}$  on the catalyst surface.

## DISCUSSION

Previous investigations have shown that the specific activity

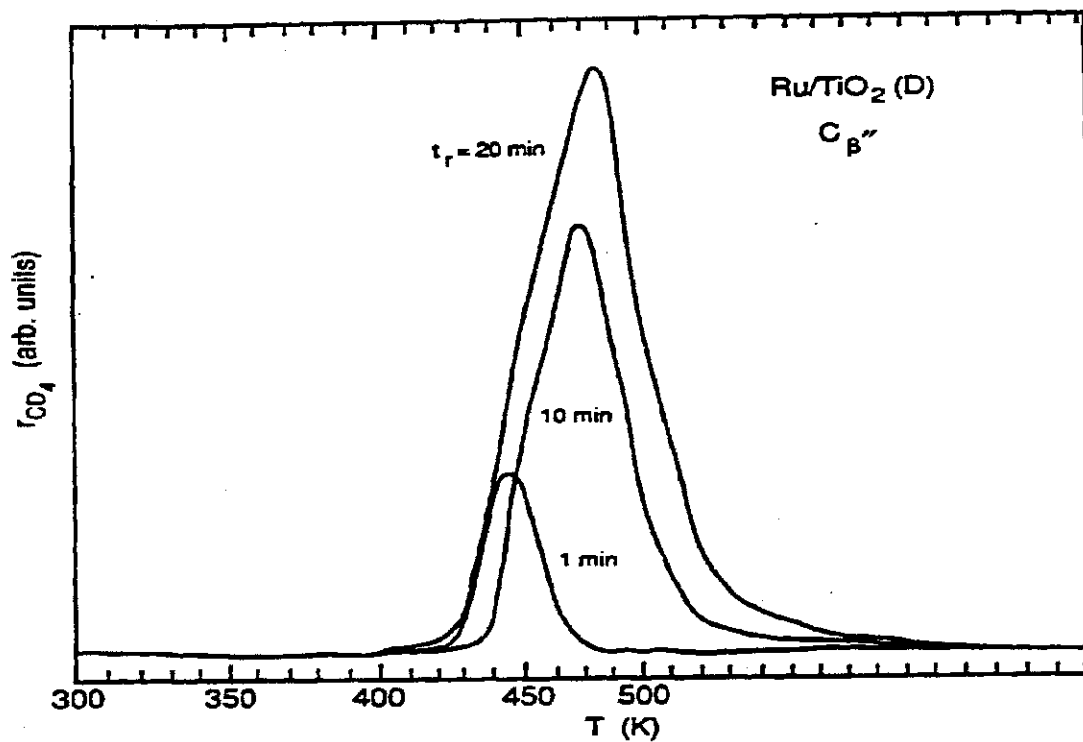


Fig. 8  $^{13}\text{C}$  TPSR spectra for  $\text{C}_{\beta''}$  with varying reaction time  $t_r$ . Gas introduction sequence:  $^{13}\text{CO} + \text{D}_2 (t_r) \rightarrow ^{12}\text{CO} + \text{D}_2 (2 \text{ min}) \rightarrow \text{He}(\text{cool}) \rightarrow \text{D}_2 (\text{TPSR})$ . In the TPSR spectra, the temperature is raised from room temperature to 503 K at 0.17 K/sec and then maintained constant at 503 K.

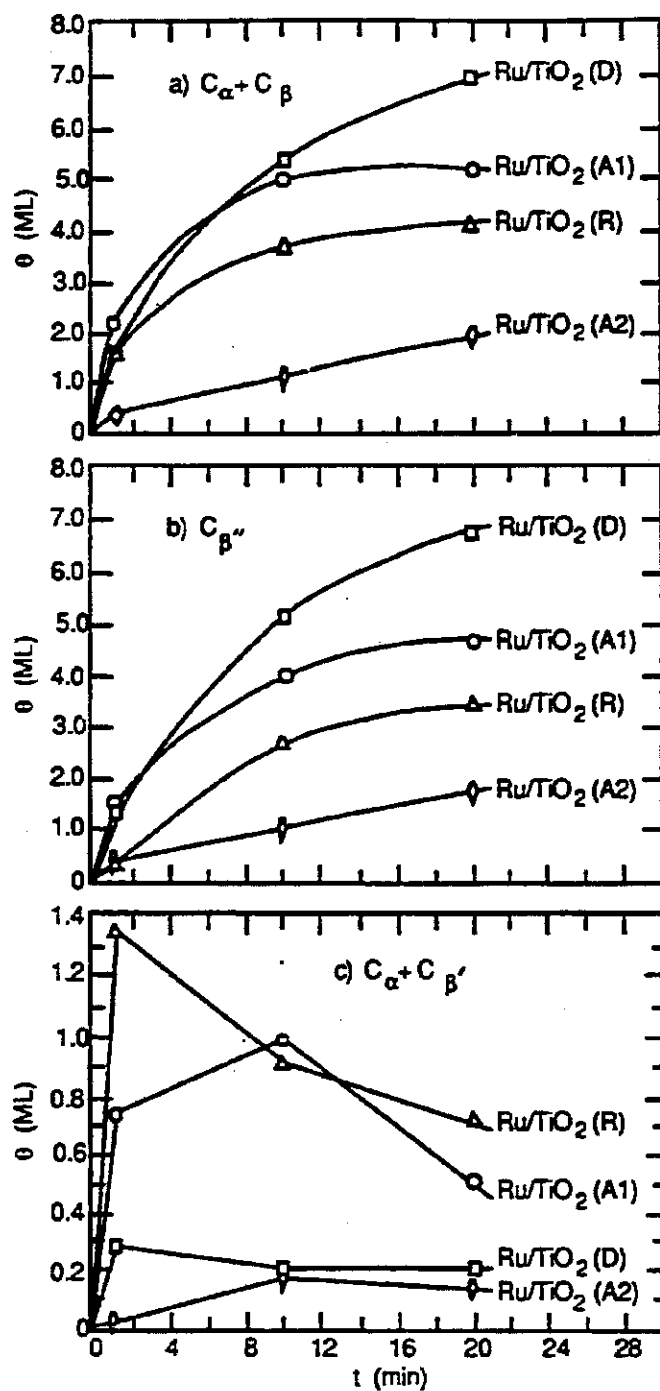


Fig. 9 Coverages of carbon species obtained from <sup>13</sup>C TPSR as a function of reaction time. a.  $C_\alpha + C_\beta$ . b.  $C_{\beta''}$ . c.  $C_\alpha + C_{\beta'}$ .

Table 4

Comparison of the time constants for the accumulation of  $C_{\alpha} + C_{\beta}$  with that for the decay in  $N_{CO}$  during the first 10 min under reaction conditions

Catalyst	$(C_{\alpha} + C_{\beta})$ (min)	$N_{CO}$ (min)
Ru/TiO <sub>2</sub> (D)	6.1	6.3
Ru/TiO <sub>2</sub> (A1)	8.3	8.7
Ru/TiO <sub>2</sub> (A2)	6.2	7.8
Ru/TiO <sub>2</sub> (R)	8.3	8.3

of Ru for Fischer-Tropsch synthesis decreases with increasing Ru dispersion (24, 25). A similar trend has been observed in the present study for the CO turnover frequency measured after 1 min and for the turnover frequency determined by extrapolation of the slowly deactivating portion of the activity versus time plots (see Fig. 1). As can be seen in Fig. 2, with the exception of the point for Ru/TiO<sub>2</sub>(R), all of the data fall along a single line, suggesting that the surface area of titania does not affect the specific activity of Ru. The deviation of the point for Ru/TiO<sub>2</sub>(R) is believed to be due to the higher chloride content of this catalyst relative to the other three. Cl impurities can inhibit the catalytic activity of Ru for CO hydrogenation (26). Iyagba et al. (26) have shown that for a fixed Ru dispersion, the turnover frequency for CO hydrogenation decreases with increasing initial levels of chloride impurity. Based on their results, it is estimated that the Cl impurity in the Ru/TiO<sub>2</sub>(R) catalyst could be expected to reduce the activity of this catalyst by about a factor of 2. This is nearly the same as the ratio of turnover frequencies for Ru/TiO<sub>2</sub>(A1) and Ru/TiO<sub>2</sub>(R), which have identical dispersions.

To determine whether the decrease in turnover frequency with increasing Ru dispersion is dependent on the support composition, a comparison was made between Ru/TiO<sub>2</sub> and Ru/Al<sub>2</sub>O<sub>3</sub> catalysts. Figure 10 shows the turnover frequencies for methane obtained in the present study and similar results obtained by Kellner and Bell (25) using Ru/Al<sub>2</sub>O<sub>3</sub> catalysts. It is evident that the slopes of the two sets of data are identical, indicating that the decrease in

turnover frequency with increasing dispersion is an intrinsic function of the Ru particle size, independent of the support composition. Figure 10 shows as well that at a fixed Ru dispersion, the methane turnover frequency is 2 times higher for titania-supported Ru than for alumina-supported Ru. Since the weight ratio of  $C_{2+}$  products to methane is roughly a factor of five higher for the titania supported catalysts, this means that the CO turnover frequency for the titania-supported catalysts is approximately a factor of ten higher than that for alumina-supported Ru.

The higher activity of  $TiO_2$ -supported Ru to  $Al_2O_3$ -supported Ru can be attributed to effects of highly active sites located at the boundaries of  $TiO_x$  islands located on the Ru metal surface. XPS studies (27) have suggested that the partial reduction of  $TiO_2$  produces  $Ti^{3+}$  sites which can then interact with the oxygen of CO adsorbed on metal atoms immediately adjacent to the  $Ti^{3+}$  ions. This mode of CO adsorption has been proposed to weaken the C-O bond, and hence facilitate its cleavage, an important first step in CO hydrogenation (28-34). The  $TiO_x$  coverage is independent of Ru dispersion.

Kellner and Bell (25) have attributed the decrease in specific activity with increasing Ru dispersion to a geometric effect. They note that an essential step in the hydrogenation of CO to hydrocarbons is the dissociation of adsorbed CO. Indirect evidence suggests that this process occurs preferentially on flat metal surfaces, rather than on low coordination sites occurring at the corners and edges of metal particles (35, 36). Since the proportion

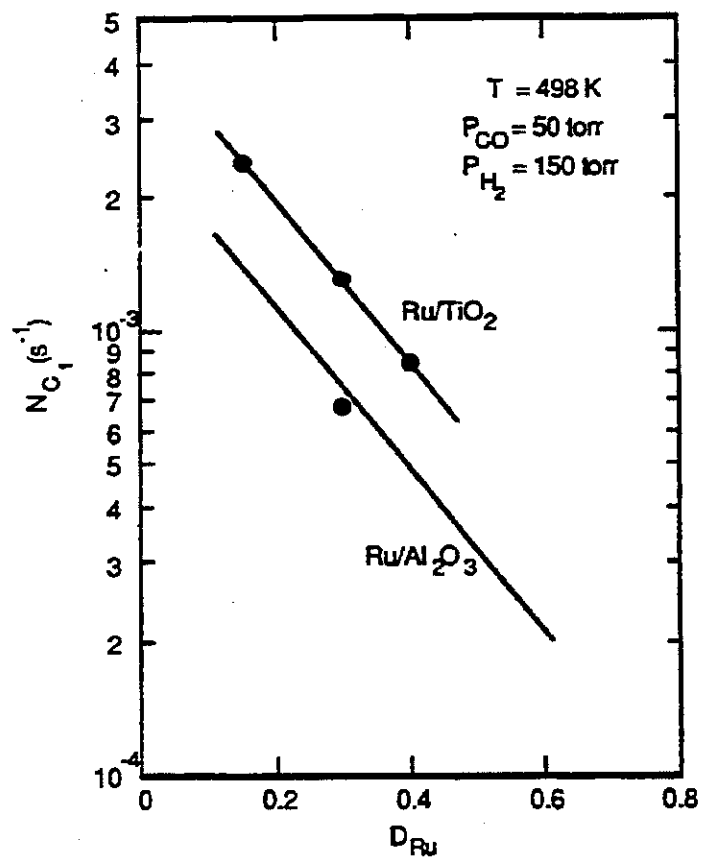


Fig. 10 Comparison of methane turnover frequency from this work over  $Ru/TiO_2$  and  $Ru/Al_2O_3$  (25). All data are based on measurements made using a  $H_2/CO$  feed mixture.

of surface metal sites occurring on flat planes decreases with increasing metal dispersion, it is possible to explain the results shown in Fig. 10. The postulation of CO dissociation as a rate-determining step in CO hydrogenation is also consistent with the observed distribution of products. As noted in the preceding section, the probability of chain growth,  $\alpha$ , is independent of Ru dispersion. This together with the absence of any effect of dispersion on the olefin to paraffin ratio or the extent of chain branching suggest that the only step in the reaction sequence affected by Ru particle size is the initial process of CO dissociation.

The importance of CO dissociation in CO hydrogenation is also borne out by the observation that the room-temperature disproportionation of CO is most extensive on the catalyst exhibiting the highest initial activity, Ru/TiO<sub>2</sub>(D), and is least extensive on the catalyst with the lowest initial activity, Ru/TiO<sub>2</sub>(R) (see Table 3). Furthermore, the observation of room-temperature CO disproportionation on Ru/TiO<sub>2</sub> indicates a higher activity for these catalysts compared to silica-supported Ni, Co, and Ru, which require temperatures of at least 423 K (37).

All four Ru/TiO<sub>2</sub> catalysts exhibit very similar deactivation behavior with time under reaction conditions. There is a very rapid loss of activity during the first 20 min or so, whereafter the activity declines much more slowly. Deactivation does not change the product carbon number distribution; the product selectivity is independent of the degree of deactivation, the dispersion of Ru, and the phase of the titania support. Comparison of the data in Figs. 1



and 6 shows that the loss in synthesis activity is accompanied by a loss in CO chemisorption capacity. Hydrogen reduction of the catalyst fully restores the initial activity of the catalysts as well as their CO chemisorption capacity. What this indicates is that the loss in activity is reversible and does not appear to be associated with a decrease in metal dispersion.

For very short reaction times ( $t_r \leq 1$  min), the loss in Ru activity can be attributed to the accumulation of  $C_\alpha$ . As noted earlier, this species is a precursor to the formation of hydrocarbons. However, the increase in coverage of  $C_\alpha$  will result in a loss in CO chemisorption capacity. This is also shown in Table 3. Hoffmann and Robbins (38) have also observed a loss in CO chemisorption capacity during CO hydrogenation over Ru (001) due to the formation of surface carbon. Figure 9c shows, though, that the coverage of  $C_\alpha + C_\beta'$  rapidly passes through a maximum with reaction time. For reaction times longer than a few minutes, the coverage by  $C_\beta''$  becomes significant, and it is probably this species which is primarily responsible for the loss in catalytic activity and CO chemisorption capacity at longer reaction times. The TPSR spectra presented in Fig. 8 indicate that  $C_\beta$  does not undergo hydrogenolysis until much of the chemisorbed CO has been removed from the surface, in agreement with earlier observations by Kobori et al. (39) and Zhou and Gulari (16). It has been proposed (16, 40, 41) that the stability of alkyl groups in the  $C_\beta''$  pool is due to the stabilization of CO adsorbed on the same, or nearby, sites. It is interesting to note

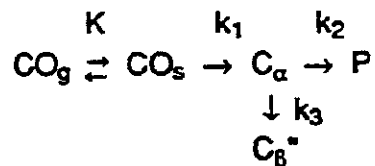
in this context that White and coworkers (40) have reported a similar stabilization of ethylidyne by adsorbed CO on a Ni(111) surface.

The loss in catalytic activity for longer reaction times is attributed to the progressive accumulation of  $C_{\alpha}$  and  $C_{\beta}$ . This explanation is suggested by the similarity in the time constants for the accumulation of  $C_{\alpha}$  and  $C_{\beta}$ , and the time constant for deactivation during the first 10 min of reaction (see Table 4). While the results of the present study do not provide direct evidence of a correlation between activity loss and the accumulation of carbon for reaction times in excess of 20 min, one can infer such a relationship from the observed correlation between the loss in CO chemisorption capacity and activity (see Table 2), since the loss in CO chemisorption capacity is ascribable to the accumulation of carbonaceous species.

Further support for the idea that the slow deactivation is due to species produced by the catalyst can be drawn from Fig. 3. This figure shows that the rate of deactivation for  $t_r > 20$  min increases linearly with the turnover frequency of the catalyst. For Ru/TiO<sub>2</sub>(D), Ru/TiO<sub>2</sub>(A1) and Ru/TiO<sub>2</sub>(A2), the differences in the turnover frequency are due to differences in Ru dispersion (see Fig. 2). As discussed above, the lower than anticipated activity of Ru/TiO<sub>2</sub>(R) is attributed to the higher initial Cl impurity of this catalyst relative to the other three investigated.

The observed pattern of deactivation and loss in CO chemisorption capacity can be represented qualitatively by the

following sequence of steps.



The first step is the reversible, nondissociative adsorption of CO. Isotopic tracer studies (8, 13, 42) have shown that this step can be assumed to be at equilibrium under reaction conditions.

Dissociation of adsorbed CO produces  $\text{C}_\alpha$ , which is viewed in the above scheme as a precursor to both hydrocarbon products and  $\text{C}_\beta^*$ .

The accumulation of  $\text{C}_\beta^*$  is assumed to reduce the fraction of metal sites available for CO adsorption and hence will inhibit the rate at which products are formed.

The general features of the proposed scheme are also supported by isotopic tracer studies conducted using Ru/SiO<sub>2</sub> (9, 11), Ru/Al<sub>2</sub>O<sub>3</sub> (15), and Ru/TiO<sub>2</sub> (14). In as much as the work carried out with Ru/TiO<sub>2</sub> (14) has shown the surface coverage by  $\text{C}_\beta^*$  to be small relative to  $\text{C}_\alpha$  and  $\text{C}_\beta^*$ , the presence of  $\text{C}_\beta^*$  is not indicated explicitly in the proposed scheme, and in the analysis of the dynamics of carbon accumulation on the catalyst surface presented below, the coverage by  $\text{C}_\beta^*$  is included implicitly with that by  $\text{C}_\alpha$ . As written, the proposed scheme assumes that the coverage of the catalyst by hydrogen is time independent. In one tracer study, Wislow and Bell (10) observed close to monolayer coverages of both CO and D<sub>2</sub> on an unsupported Ru catalyst under reaction conditions,

indicating that CO and D<sub>2</sub> chemisorb on different sites.

Expressions for the rate of product formation and for the coverage of the catalyst surface by CO, C<sub>α</sub>, and C<sub>β</sub><sup>\*</sup> can be derived on the basis of the reaction scheme presented above. The rate of product formation can be expressed as

$$N_{CO} = k_2\theta_\alpha \quad (1)$$

The coverage of the surface by CO, C<sub>α</sub>, and C<sub>β</sub><sup>\*</sup> is governed by the following relationships

$$\theta_{CO} = \frac{KP_{CO}(1-\theta_\alpha-\theta_\beta^*)}{1+KP_{CO}} \quad (2)$$

$$\frac{d\theta_\alpha}{dt} = k_1\theta_{CO} - (k_2+k_3)\theta_\alpha \quad (3)$$

$$\frac{d\theta_\beta^*}{dt} = k_3\theta_\alpha \quad (4)$$

where  $\theta_{CO}$ ,  $\theta_\alpha$ , and  $\theta_\beta^*$  are the coverages of CO, C<sub>α</sub>, and C<sub>β</sub><sup>\*</sup>, respectively; P<sub>CO</sub> is the partial pressure of CO; K is the equilibrium constant for CO adsorption; and k<sub>i</sub> is the rate coefficient for reaction i. The initial conditions for eqns. 3 and 4 are  $\theta_\alpha = \theta_\beta^* = 0$ .

Assuming that  $KP_{CO} \gg 1$ , the time dependences of  $\theta_\alpha$  and  $\theta_\beta^*$  are given by

$$\theta_{\alpha}(t) = \frac{k_1(\exp(m_1 t) - \exp(m_2 t))}{\sqrt{(k_1 + k_2 + k_3)^2 - 4k_1 k_3}} \quad (5)$$

and

$$\theta_{\beta}''(t) = 1 + \frac{k_1 k_3 \left( \frac{\exp(m_1 t)}{m_1} - \frac{\exp(m_2 t)}{m_2} \right)}{\sqrt{(k_1 + k_2 + k_3)^2 - 4k_1 k_3}} \quad (6)$$

where

$$m_{1,2} = \frac{-(k_1 + k_2 + k_3) \pm \sqrt{(k_1 + k_2 + k_3)^2 - 4k_1 k_3}}{2} \quad \text{and } m_1 > m_2$$

Substitution of eqns. 5 and 6 into eqn. 2 gives

$$\theta_{CO}(t) = \frac{k_1}{\sqrt{(k_1 + k_2 + k_3)^2 - 4k_1 k_3}} \left( \exp(m_2 t) \left( 1 + \frac{k_3}{m_2} \right) - \exp(m_1 t) \left( 1 + \frac{k_3}{m_1} \right) \right) \quad (7)$$

and

$$\frac{N_{CO}(t)}{\theta_{CO}(t)} = \frac{k_2(\exp(m_1 t) - \exp(m_2 t))}{\left( \exp(m_2 t) \left( 1 + \frac{k_3}{m_2} \right) - \exp(m_1 t) \left( 1 + \frac{k_3}{m_1} \right) \right)} \quad (8)$$

Plots of  $N_{CO}/\theta_{CO}$ ,  $\theta_{CO}$ ,  $\theta_{\alpha}$ , and  $\theta_{\beta}''$  are shown in Fig. 11. The values of the three rate coefficients used to generate these plots were selected to be representative of the dynamics observed in the experiments reported here. Comparison of the curves shown in Fig. 11 with the data shown in Figs. 6 and 9 shows a number of similarities. The coverage of CO decreases very rapidly during the first two to three minutes and then decays more slowly. This

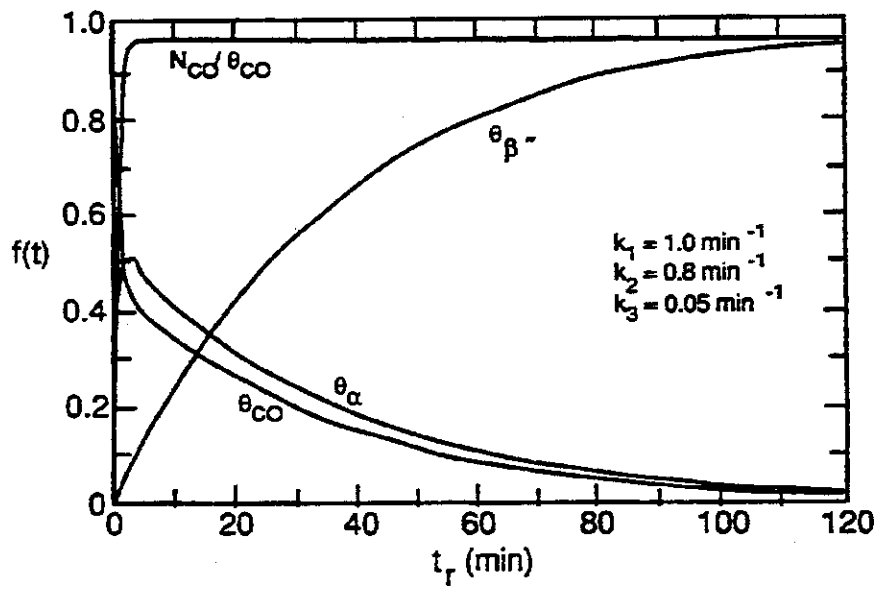


Fig. 11 Model curves for  $N_{CO}/\theta_{CO}$ ,  $\theta_{\alpha}$ ,  $\theta_{CO}$ , and  $\theta_{\beta^*}$  as a function of reaction time.

pattern can be attributed to the rapid initial build up of  $(C_{\alpha} + C_{\beta}')$  and the subsequently slower build up of  $C_{\beta}''$ . In agreement with experimental observation, the coverage by  $(C_{\alpha} + C_{\beta}')$  passes through a maximum within the first few minutes of reaction, whereas the coverage by  $C_{\beta}''$  rises monotonically. The ratio  $N_{CO}/\theta_{CO}$  rises rapidly to a fixed value which remains constant thereafter, in agreement with the observation that  $N_{CO}$  and  $\theta_{CO}$  decline concurrently at  $t_r \geq 10$  minutes.

The proposed model assumes that hydrogen chemisorption is not affected by the process of reaction and subsequent slow reduction in adsorbed CO on the catalyst surface. There is also an implicit assumption in the model that the chain length of the  $C_{\beta}''$  is time independent. Analysis of our data indicates that the ratio of the average chain length of the accumulated carbon at 10 min of reaction to that at 1 min after the start-up of reaction is  $2.8 \pm 0.6$ , while the ratio estimated between 20 min and 10 min is only  $1.3 \pm 0.3$ . This indicates that the average chain length rises rapidly and then at a slower rate as reaction proceeds. A similar pattern has also been observed recently by Zhou and Gulari (16) for Ru/Al<sub>2</sub>O<sub>3</sub>. One can, therefore, envision a scenario in which the number of Ru surface sites blocked by each unit of  $C_{\beta}''$  decreases with time. During a period of rapidly increasing chain length (i. e., shortly after the start-up of reaction) the assumption of a constant chain length would lead to an overestimation of the effects of  $C_{\beta}''$  accumulation and, hence, to an underestimation in  $\theta_{CO}$ . Despite these simplifying

assumptions, the model does qualitatively describe experimental observations.

Finally, one might ask whether the observed loss in activity might be due to the progressive accumulation of wax either on the surface of Ru particles or in the catalyst pores. To address this question, estimates were made of the wax accumulation after 2 h of reaction. The carbon number threshold for condensation of wax was determined using an extrapolation of the measured ASF distribution together with the Kelvin equation and known vapor pressures of alkanes. For the conditions of the present experiments, it was found that all products with 28 carbon atoms or more would condense in 10 Å pores, whereas all products with 83 carbon atoms or more would condense in 100 Å pores. The total wax accumulation could then be calculated for each catalyst using the measured pore size distribution. By this means, it was found that the wax could occupy between 0.06-0.55% of the pore volume in the four catalysts studied. If the wax is assumed to cover the Ru particles in a maximal fashion, then it is estimated that between 3% and 7% of the exposed Ru sites would be covered. These figures are to be compared with fractional activity losses of 23-46% over the same period of time. This suggests that wax accumulation cannot account for a significant part of the loss in activity under the conditions used in this study. Of further note is the fact that the estimated amount of wax accumulation is only 1-4% of the amount of carbon removed from the catalyst surface after reaction.



## CONCLUSIONS

Titania-supported Ru catalysts undergo deactivation during CO hydrogenation, but exhibit no change in product selectivity with time onstream. The initial activity can be restored by reduction in H<sub>2</sub> or D<sub>2</sub> and there is no evidence of metal sintering due to reaction. The rate of deactivation is most rapid during the first 20 min after the startup of reaction and declines to a much smaller rate for reaction times longer than 20 min. The long-term rate of deactivation is proportional to the activity of the catalyst, obtained by extrapolation of the long-term activity data. The loss in activity is paralleled by a loss in CO chemisorption capacity, and for reaction times longer than 20 min, the ratio of the CO turnover frequency to the CO coverage remains constant. Differences in the initial activity of Ru supported on Degussa P-25 and anatase can be attributed to differences in Ru dispersion, with higher dispersion contributing to a decrease in CO turnover frequency. For the same dispersion, Ru supported on rutile exhibits a two to threefold lower activity than Ru supported on anatase. The lower activity of rutile-supported Ru is attributed to the higher level of chloride impurity on rutile versus anatase. The formation of highly active sites at the boundaries of TiO<sub>x</sub> islands located on the metal surface is proposed to be the cause for the higher activity of TiO<sub>2</sub>-supported Ru, compared to SiO<sub>2</sub>- or Al<sub>2</sub>O<sub>3</sub>-supported Ru.

Temperature-programmed surface reaction experiments show evidence of the accumulation of carbidic, C<sub>α</sub>, and alkyl, C<sub>β</sub>, carbon on

the catalyst surface. The catalyst inventory of  $(C_{\alpha} + C_{\beta}^*)$  increases, passes through a maximum, and then decreases as the catalyst loses activity. On the other hand, the inventory of  $C_{\beta}^*$  increases monotonically with reaction time. The accumulation of both  $C_{\alpha}$  and  $C_{\beta}$  carbon results in a reduction in the CO chemisorption capacity of the catalyst. The immediate loss in CO uptake after reaction start-up is attributed to the buildup of  $C_{\alpha}$ . The rapid loss in activity in the first ten minutes correlates with the buildup of  $C_{\alpha}$  and  $C_{\beta}$ , whereas the slower loss in activity is ascribed to the accumulation of  $C_{\beta}^*$ . The alkyl chains comprising the  $C_{\beta}$  pool of carbon do not undergo extensive hydrogenolysis under reaction conditions, very likely due to inaccessibility of the chains to hydrogen as a result of CO adsorbed on adjacent sites. A model has been proposed that qualitatively agrees with the experimental observations of changes in activity, CO uptake, and the accumulation of reactive and unreactive carbon species on the catalyst surface as reaction proceeds.

#### REFERENCES

1. Dalla Betta, R. A., Piken, A. G., and Shelef, M., *J. Catal.* **35**, 54 (1974).
2. Dalla Betta, R. A., Piken, A. G., and Shelef, M., *J. Catal.* **40**, 173 (1975).
3. Everson, R. C., Woodburn, E. T., and Kirk, A. R. M., *J. Catal.* **53**,

- 186 (1978).
4. Ekerdt, J. G., and Bell, A. T., *J. Catal.* **58**,170 (1979).
  5. Moeller, A. D., and Bartholomew, C. H., *Ind. Eng. Chem. Prod. Res. Dev.* **21**, 390 (1982).
  6. Bowman, R. M., and Bartholomew, C. H., *Appl. Catal.* **7**,179 (1983).
  7. Yamasaki, H., Kobori, Y., Naito, S., Onishi, T., and Tamaru, K., *J. Chem. Soc., Far. Trans.* **177**, 2913 (1981).
  8. Cant, N. W., and Bell, A. T., *J. Catal.* **73**, 257 (1982).
  9. Winslow, P., and Bell, A. T., *J. Catal.* **86**, 158 (1984).
  10. Winslow, P., and Bell, A. T., *J. Catal.* **91**, 142 (1985).
  11. Duncan, T. M., Winslow, P., and Bell, A. T., *J. Catal.* **93**, 1 (1985).
  12. Duncan, T. M., Reimer, J. A., Winslow, P., and Bell, A. T., *J. Catal.* **93**, 305 (1985).
  13. Winslow, P., and Bell, A. T., *J. Catal.* **94**, 385 (1985).
  14. Yokomizo, G. H., and Bell, A. T., *J. Catal.* **119**, 467 (1989).
  15. Zhou, X., and Gulari, E., *J. Catal.* **105**, 499 (1987).
  16. Zhou, X., and Gulari, E., *Langmuir* **4**, 1132 (1988).
  17. Kikuchi, E., Matsumoto, N., Takahashi, T., Machino, A., and Morita, Y., *Appl. Catal.* **10**, 251 (1984).
  18. Parfitt, G. D., *Trans. Far. Soc.* **67**, 2469 (1971).
  19. Tauster, S. J., Fung, S. C., and Garten, R. L., *J. Amer. Chem. Soc.* **100**, 170 (1978).
  20. Dalla Betta, R. A., *J. Catal.* **34**, 57 (1974).
  21. Taylor, K. C., *J. Catal.* **38**, 299 (1975).
  22. Kubicka, H., *React. Kin. Cat. Lett.* **5**, 223 (1976).
  23. Anderson, R. B., in "The Fischer-Tropsch Synthesis," Academic

- Press, New York, 1984.
24. King, D. L., *J. Catal.* **61**, 77 (1980).
  25. Kellner, C. S., and Bell, A. T., *J. Catal.* **75**, 251 (1982).
  26. Iyagba, E. J., Hoost, T. E., Nwalor, J. U., and Goodwin, J. G., *J. Catal.* **123**, 1 (1990).
  27. Levin, M. E., Salmeron, M., Bell, A. T., and Somorjai, G. A., *Surf. Sci.* **195**, 429 (1988).
  28. Bracey, J. D., and Burch, R., *J. Catal.* **86**, 384 (1984).
  29. Anderson, J. B. F., Bracey, J. D., Burch, R., and Flambard, A. R., "Proceedings, 8th International Congress on Catalysis," Vol V, p. 111. Berlin, 1984.
  30. Sachtler, W. M. H., in "Proceedings, 8th International Congress on Catalysis," Vol V, p.151. Berlin, 1984.
  31. Sachtler, W. M. H., Shriver, D. F., Hollenberg, W. B., and Long, A. F., *J. Catal.* **92**, 429 (1985).
  32. Vannice, M. A., and Sudhakar, C., *J. Phys. Chem.* **88**, 2429 (1984).
  33. Rieck, J. S., and Bell, A. T., *J. Catal.* **99** 262 (1986).
  34. Levin, M. E., Salmeron, M., Bell, A. T., and Somorjai, A. T., *J. Catal.* **106**, 401 (1987).
  35. Boudart, M., and McDonald, M. A., *J. Phys. Chem.* **88**, 2185 (1984).
  36. Rieck, J. S., and Bell, A. T., *J. Catal.* **103**, 46 (1987).
  37. Rabo, J. A., Risch, A. P., and Poutsma, M. L., *J. Catal.* **53**, 295 (1978).
  38. Hoffmann, F. M., and Robbins, J. L., in "Proceedings of the 9th International Congress in Catalysis, Calgary, 1989", Vol. 3,

- p.1144. Calgary, 1989.
39. Kobori, Y., Yamasaki, H., Naito, S., Onishi, T., and Tamaru, K., *J. Chem. Soc., Far. Trans. 1* **78**, 1473 (1982).
  40. Akhter, S., and White, J. M., *Surf. Sci.* **180**, 19 (1987).
  41. Akhter, S., Henderson, M. A., Mitchell, G. E., and White, J. M., *Langmuir* **4**, 246 (1988).
  42. Biloen, P., Helle, J.N., van den Berg, F. G. A., and Sachtler, W. M. H., *J. Catal.* **81**, 450 (1983).